[7] F. W. Chang, "Transient analysis of lossless coupled transmission lines in a homogeneous dielectric medium," *IEEE Trans. Microwave Theory Tech.*, vol. 18, pp. 616–626, Sept. 1970.
[8] K. D. Marx, "Propagation modes, equivalent circuits and characteristic terminations for multiconductor transmission lines with inhomogeneous dielectrics," *IEEE Trans. Microwave Theory Tech.*, vol. 21, pp. 450–457, July 1973.
[9] V. K. Tripathi and J. B. Retting, "A SPICE model for multiple coupled microstrips and other transmission lines," *IEEE Trans. Microwave Theory Tech.*, vol. 33, pp. 1513–1518, Dec. 1985.
[10] T. C. Edwards, *Foundations for Microstrip Circuit Design.* New York: Wiley, 1981.

# Spectral Analysis Considerations Relevant to Radiation and Leaky Modes of Open-Boundary Microstrip Transmission Line

Jerry Michael Grimm and Dennis P. Nyquist

***Abstract*—The continuous radiation spectrum of open microstrip transmission line and its nonspectral leaky modes are conceptualized through a transform-domain integral-operator formulation and relevant spectral analysis. Two complex (transform-variable) wavenumber planes are implicated by Sommerfeld-integral representations of associated Green's functions and the necessary axial inverse transformation to the space domain. The radiation spectrum is identified with branch cuts in the axial wavenumber plane, which constrain the migration of branch-point singularities in the transverse wavenumber plane. Leaky-wave modes occur only when the branch cuts in the axial wavenumber plane are violated, allowing branch points in the transvere wavenumber plane to migrate across the (initial) real-axis integration path. The relation between spectral radiation modes, nonspectral leaky-wave modes and branch cuts in the axial wavenumber plane is discussed. The influence of branch cuts in the axial wavenumber plane upon the location of branch points in the transverse wavenumber plane is detailed, and a rationale is offered for the choice branch cuts in the latter plane. Although the formulation is developed specifically for the microstrip line, it is applicable more generally to a wide class of open conducting or dielectric waveguides. It is believed that the ideas presented here are new and significant, and provide perhaps the first general method for conceptualizing the continuous spectrum of practical open waveguides.**

## I. Introduction

Open-boundary waveguiding systems support not only a finite number of discrete propagation modes but also a continuum of radiation modes. Knowledge of these radiation modes is vital for determination of losses due to radiation at circuit discontinuities, scattering and mode-conversion from adjacent obstacles, and coupling into other nearby open-boundary structures [1], [2]. Unfortunately, the radiation spectrum of most practical open-boundary waveguides, e.g. microstrip transmission lines, remains undetermined. This has not deterred the analysis of radiation effects from microstrip transmission lines, in which the continuous radiation spectrum contribution is approximated by the leaky-wave modes of the transmission line. Leaky-wave modes are discrete modes that possess nonspectral behavior (exponentially increasing amplitudes in the transverse plane) and are not part of the proper modal spectrum. When the Steepest Descent Contour (SDC) integration technique is used, the SDC sweeps through poles associated with these nonspectral modes (the leaky-wave poles) for restricted spatial regimes; in these regimes, the leaky-wave modes approximate the continuous radiation spectrum. Consequently, the determination of the leaky-wave modes of microstrip transmission lines has received much attention [3]–[5].

Manuscript received Jan. 10, 1992; revised Apr. 27, 1992. This research was supported in part by NSF grant ECS-86-11 958,
The authors are with the Department of Electrical Engineering, Michigan State University, East Lansing, MI 48824-1226.
IEEE Log Number 9204015.

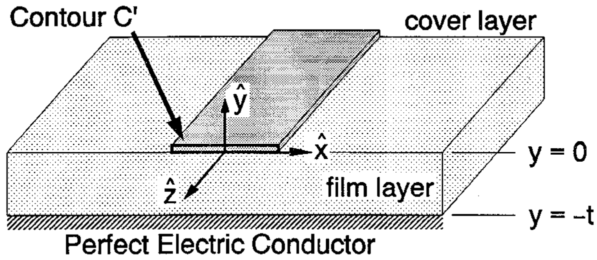


Fig. 1. Typical microstrip structure.

This paper will present a rationale for the specification of the radiation spectrum associated with microstrip transmission lines, and will address the issue of determining the leaky-wave modes of those structures.

## II. Development of Relevant Green's Functions

The configuration of interest is shown in Fig. 1. The microstrip transmission line lies at the cover-film interface in the cover region of a tri-layered, planar dielectric background environment. The cover layer is assumed to be semi-infinite in vertical extent, while the film layer has a finite thickness and is backed by a perfect electric conductor. The layer interfaces are assumed to be infinite in transverse extent, and each layer is homogeneous. A coordinate system is chosen such that the $x$ and $z$ axes are tangential to the planar interfaces, while $y$ is normal to those interfaces.

A field incident upon the microstrip structure induces surface currents; these in turn support a scattered field. By satisfying the boundary conditions at the surface of the microstrip, an electric field integral equation (EFIE), formulated in terms of electric Hertzian potentials $\vec{\Pi}(\vec{r})$ supported by the induced surface currents $\vec{K}(\vec{r})$, can be constructed as

$$\hat{t} \cdot (k_c^2 + \nabla\nabla\cdot) \int_{s'} \overleftrightarrow{G}(\vec{r}|\vec{r}') \cdot \frac{\vec{K}(\vec{r}')}{j\omega\epsilon_c} dl' = -\hat{t} \cdot \vec{E}^{\mathrm{inc}}(\vec{r}); \qquad \forall \vec{r} \in S. \tag{1}$$

Uniformity of the background environment parallel to the $x$–$z$ plane prompts application of a two-dimensional spatial Fourier transform on the coordinates tangential to the interfaces, defined as

$$\vec{\Pi}(\vec{r}) = \frac{1}{(2\pi)^2} \int_{-\infty}^{\infty} \int_{-\infty}^{\infty} \tilde{\Pi}(y; \vec{\lambda}) e^{j\vec{\lambda}\cdot\vec{r}} d^2\lambda$$
$$\tilde{\Pi}(y; \vec{\lambda}) = \int_{-\infty}^{\infty} \int_{-\infty}^{\infty} \vec{\Pi}(\vec{r}) e^{-j\vec{\lambda}\cdot\vec{r}} d^2 r \tag{2}$$

where $\vec{\lambda} = \hat{x}\xi + \hat{z}\zeta, \lambda^2 = \xi^2 + \zeta^2, d^2\lambda = d\xi d\zeta$, and $\xi$ and $\zeta$ are generally complex-valued spatial frequencies corresponding to the $x$ and $z$ spatial variables. The necessary Green's function can easily be determined in the transform domain [6]; a subsequent two-dimensional inverse transformation will recover the space domain quantities.

The uniformity and infinite extent of the microstrip line in the axial direction ($z$) renders EFIE (1) convolutional in nature, since $\overleftrightarrow{G}(\vec{r}|\vec{r}') = \overleftrightarrow{G}(\vec{\rho}|\vec{\rho}'; z - z')$ with $\vec{\rho}$ the 2-D transverse position vector. This prompts an axial Fourier transformation, and the propagation mode spectrum is consequently defined by the equivalent axial transform-domain EFIE

$$\hat{t} \cdot (k_c^2 + \tilde{\nabla}\tilde{\nabla}\cdot) \oint_{C'} \overleftrightarrow{g}(\vec{\rho}|\vec{\rho}'; \zeta) \cdot \frac{\vec{k}(\vec{\rho}'; \zeta)}{j\omega\epsilon_c} dl' = -\hat{t} \cdot \vec{e}^{\,\mathrm{inc}}(\vec{\rho}; \zeta); \qquad \forall \vec{\rho} \in C \tag{3}$$

where $\zeta$ is the axial transform variable, $\tilde{\nabla} = \hat{x}\partial/\partial x + \hat{y}\partial/\partial y + \hat{z}j\zeta$, $\vec{k}(\vec{\rho}; \zeta)$ is surface current in the axial transform domain, $C'$ is the cross-section contour and $\overleftrightarrow{g}(\vec{\rho}|\vec{\rho}'; \zeta)$ is a dyadic Green's function for the transformed Herztian potentials, appropriately specialized to the background environment. Subsequent to the determination of $\vec{k}(\vec{\rho}; \zeta)$, an inverse Fourier transform on $\zeta$ is performed to recover the spatial current $\vec{K}(\vec{r})$. The appropriate Green's dyadic decomposes into two components—a principal dyadic, denoted as $\overleftrightarrow{g}^p$, which describes the potential maintained by the surface currents radiating in an unbounded medium, and a reflected dyadic, denoted as $\overleftrightarrow{g}^r$, which describes the influence of the multi-layered background structure on that principal potential. As detailed in [6], the Green's dyadic in the axial-transform domain takes the form

$$\overleftrightarrow{g}(\vec{\rho}|\vec{\rho}'; \zeta) = \overleftrightarrow{I}\, g^p + \left[ (\hat{x}\hat{x} + \hat{z}\hat{z}) g_t^r + \hat{y}\left( \frac{\partial}{\partial x} g_c^r \hat{x} + g_n^r \hat{y} + j\zeta g_c^r \hat{z} \right) \right] \tag{4}$$

with the scalar components of (4) having the Sommerfeld-integral representations

$$g^p(\vec{\rho}|\vec{\rho}'; \zeta) = \int_{-\infty}^{\infty} \frac{e^{-p_c|y-y'|}}{4\pi p_c} e^{j\xi(x-x')} d\xi \tag{5}$$

$$\begin{Bmatrix} g_t^r(\vec{\rho}|\vec{\rho}'; \zeta) \\ g_n^r(\vec{\rho}|\vec{\rho}'; \zeta) \\ g_c^r(\vec{\rho}|\vec{\rho}'; \zeta) \end{Bmatrix} = \int_{-\infty}^{\infty} \begin{Bmatrix} R_t(\lambda) \\ R_n(\lambda) \\ C(\lambda) \end{Bmatrix} \frac{e^{-p_c(y+y')}}{4\pi p_c} e^{j\xi(x-x')} d\xi. \tag{6}$$

Wavenumber parameters $p_i = \sqrt{\lambda^2 - k_i^2}$ ($i = c, f$ for cover or film, respectively) arise from the transformed Helmholtz equation for Hertzian potentials, while reflection and coupling coefficients $R_t, R_n$ and $C$ depend upon details of the background environment through the $p_i$ and possess denominators which give rise to pole singularities in the complex $\xi$-plane. The Green's functions are one-dimensional inverse Fourier transforms on the transverse spatial frequency $\xi$.

The quantity $p_i$ is multivalued, making branch cuts in the complex $\xi$-plane necessary to render the integrands in (5) and (6) analytic. For the microstrip transmission line under consideration, only the branch point associated with $p_c$ is implicated (the branch points associated with $p_f$, at $\lambda = \pm k_f$, are removable) and branch points occur at $\lambda = \pm k_c$. Branch cuts are chosen by enforcing the Sommerfeld radiation condition; this leads to the well-known hyperbolic cuts in the Sommerfeld (complex-$\lambda$) plane [7], [8]. But, since $\lambda^2 = \xi^2 + \zeta^2$, it is apparent that the necessary branch cuts for representations (5) and (6) are not independent of the cutting of the axial transform (complex-$\zeta$) plane, but rather are related to one another and the unambiguous cutting of the Sommerfeld plane.

## III. Cutting of the Complex $\zeta$-Plane

The previous efforts [1]–[3] on the propagation-mode spectrum of microstrip have failed to specify an explicit branch cut in the complex $\zeta$-plane. This oversight is readily explained. The transform-domain current is found [9] to possess simple pole singularities at $\zeta = \pm\zeta_p$, which naturally leads to the discrete propagation modes. Those modes arise from residue contributions to the inverse transform on $\zeta$ when recovering the space domain current. The discrete-mode current will take the form of $\vec{K}_D^{\pm}(\vec{r}) = U[\pm(z - z')]A_D^{\pm}\vec{k}_D^{\pm}(\vec{\rho})e^{\mp j\zeta_p z}$, where $\vec{k}_D^{\pm}(\vec{\rho})$ satisfies the homogeneous specialization of EFIE (3). Quantification of the discrete modes is typically terminated at this point. However, the process of recovering the discrete modes through the axial inverse transform, though trivial, assumes that the transform-domain current remains analytic in the complex $\zeta$-plane, an assumption that cannot be guaranteed until a branch cut in the complex $\zeta$-plane is specified.

A rationale for the $\zeta$-plane branch cut is suggested by considering the form of the principal Green's function (5). This is the Green's function for an unbounded homogenous medium, and the inverse transform can be performed analytically, resulting in the familiar two-dimensional form of

$$g^p(\vec{\rho}|\vec{\rho}'; \zeta) = \tfrac{1}{2} K_0\left(\sqrt{\zeta^2 - k_c^2}|\vec{\rho} - \vec{\rho}'|\right) \tag{7}$$

where $K_0$ is the modified Bessel function of the second kind. Note that representation (7) possesses an explicit square-root dependence upon $\zeta$, leading to branch points at $\zeta = \pm k_c$. Assuming small material losses ($k_c = k_{cr} + jk_{ci}, k_{ci} < 0$), enforcement of the Sommerfeld radiation condition requires $\mathcal{R}e\{\sqrt{\zeta^2 - k_c^2}\} > 0$ leading to the conclusion that

$$-\frac{\pi}{2} < \mathrm{Arg}\{\sqrt{\zeta^2 - k_c^2}\} \leq \frac{\pi}{2}. \tag{8}$$

The branch cut which satisfies the restrictions in inequality (8) is hyperbolic in the complex $\zeta$-plane, initiating at the branch points of $\zeta = \pm k_c$, and extending asymptotically to infinity along the imaginary axis, such that

$$\zeta_b = \frac{k_{cr}k_{ci}}{\zeta_i} + j\zeta_i; \qquad |\zeta_i| > |k_{ci}|. \tag{9}$$

This branch cut separates the spectral and nonspectral (top and bottom Riemann) sheets in the complex $\zeta$-plane, and is shown in Fig. 2(a). Since the reflected Green's functions arise from the principal Green's function (reflection of the principal wave), they share the same branch points at $\zeta = \pm k_c$ and the branch cut in defined in (9).

Another rationale for choosing the $\zeta$-plane branch cut can be obtained by considering the location and migration of the $\xi$- plane branch points associated with $p_c$. Occurring when the argument of $p_c$ is zero, the branch points in the $\xi$-plane are located where $\xi_B^2 = k_c^2 - \zeta^2$, or

$$\xi_B = -j\sqrt{\zeta^2 - k_c^2} = -j\sqrt{\zeta - k_c}\sqrt{\zeta + k_c}. \tag{10}$$

The location of $\xi_B$ is again defined through a square root, thus requiring a branch cut in the complex $\zeta$-plane to maintain analyticity. The branch points $\xi = \pm\xi_B$ are fixed for the spectral $\xi$-plane integration; however, as the value of $\zeta$ varies, it is apparent from (10) that the $\xi$- plane branch points will migrate. This can be potentially disastrous, as migration of the branch points across the real-line inversion contour in the $\xi$-plane will lead to discontinuous physical phenomena and nonspectral behavior. To uniquely locate the $\xi$-plane branch points in the upper/lower half plane, it is necessary to require that $\mathcal{I}m\{\xi_B\} < 0$, which in turn leads to

$$\mathcal{R}e\{\sqrt{\zeta^2 - k_c^2}\} > 0. \tag{11}$$

This latter condition in relation (11) exactly replicates that in (8), thus leading to precisely the same hyperbolic cuts in the complex $\zeta$-plane as given in relation (9). This alternative rationale is based upon physical wave phenomena, and represents a major contribution of this paper.

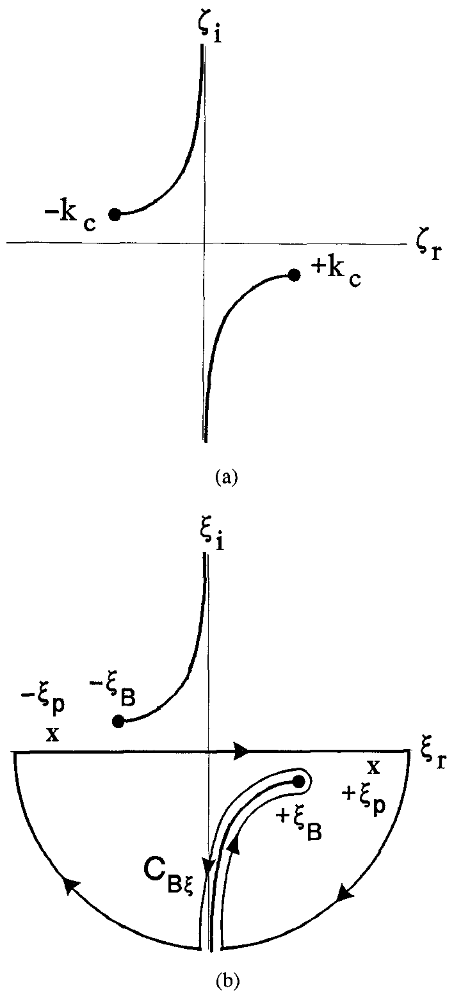


Fig. 2. (a) Branch cut necessary in the $\zeta$-plane to restrict $\xi$-plane branch point migration. (b) Mapping of Sommerfeld-plane branch cuts into the $\xi$-plane for proper modes of the microstrip, and illustration of the contour deformation used for evaluation of the Green's function representations (case of $x < x'$).

Upon determining the branch cut in the $\zeta$-plane, the three-dimensional spatial microstrip surface current can be represented as

$$\vec{K}(\vec{\rho}, z) = \pm jU\big(\pm[z - z']\big) \sum_{p=1}^{N} a_p^{\pm} \vec{k}^{\pm}(\vec{\rho}; \zeta_p) e^{\mp j\zeta_p z} - \frac{1}{2\pi} \int_{C_{B\pm}} \vec{k}(\vec{\rho}; \zeta) e^{j\zeta z} d\zeta \qquad (12)$$

where $\vec{k}(\vec{\rho}; \zeta)$ is the solution to the forced transform-domain EFIE (3) and $C_B$ is the contour deformed about both sides of the branch cut in the complex $\zeta$-plane. This is a spectral superposition of all discrete axial eigencurrents of the structure plus the contribution of the axial radiation spectrum. The formulation in (12) is applicable for modal decomposition in the anlaysis of scattering, coupling, or excitation of EM waves along the open-boundary microstrip structure.

## IV. Consequences and Relation to Leaky Modes

Choice of description (9) for the branch cut in the complex $\zeta$-plane has direct consequences on evaluation of the inverse $\xi$-transforms which define the Green's functions in representations (5) and (6); as the value of $\zeta$ changes, the locations of all the singularities in the complex $\xi$-plane migrate. The most important consequence is that the $\xi$-plane branch point $\xi_B$ of $p_c$, as described above, is confined to the lower half of the complex $\xi$-plane. The branch cuts in the $\xi$-plane are simple mappings of those in the Sommerfeld $\lambda$-plane through $\xi^2 = \lambda^2 - \zeta^2$ for any given $\zeta$. For any point on the spectral (upper) sheet of the $\zeta$-plane, the $\xi$-plane branch cuts take on the familiar hyperbolic shape (Fig. 2(b) and separate the spectral sheet of the $\xi$-plane from the nonspectral one. Once the $\xi$-plane cutting is determined, the residues of the pole singularities in the integrands, arising from the zeros in the denominators of reflection and coupling coefficients $R_T, R_N$ and $C$, are easily determined, providing that this is done in a manner consistent with the $\xi$-plane cutting. Once all the complex $\xi$- plane singularities are determined, contour deformation in the $\xi$-plane can be performed to evaluate the Green's functions, resulting in the general forms

$$g_\beta^\alpha(\vec{\rho}|\vec{\rho}'; \zeta) = \pm j \sum_{n=1}^{N} \mathrm{Res}\{f_\beta^\alpha(y, y', \zeta, \xi)\}|_{\mp\xi_n} e^{-j\xi_n|x-x'|} \pm \frac{1}{2\pi} \int_{C_{B,\xi}} f_\beta^\alpha(y, y', \zeta, \xi) e^{-j\xi_n|x-x'|} d\xi \qquad (13)$$

where $g_\beta^\alpha$ is any scalar Green's function component in representation (5) and (6) and $\pm$ refers to upper/lower half-plane closure for $x > x'$ or $x < x'$, respectively. Another consequence of working with the spectral modes of the transmission line is that leaky-wave poles of the background environment are never implicated.

Leaky wave modes for the microstrip transmission line can be found by intentionally violating the branch cut defined by (9). The most immediate consequence is that the branch point of $p_c$ in the $\xi$-plane ($+\xi_B$) will migrate from the lower half-plane (LHP) to the upper half-plane (UHP). This migration forces the real-line inversion contour in the $\xi$-plane to be deformed, remaining above the original LHP singularities, such that the forward transform on $x$ remains convergent [10], [12]. This is equivalent to Chew's argument that continuity of the physical problem must be maintained [11]. Branch cuts in the $\xi$-plane still must be specified. When $\xi_B$ migrates from LHP to UHP, an attempt to map the Sommerfeld-plane branch cut to the $\xi$-plane through the relationship $\xi^2 = \lambda^2 - \zeta^2$ results in a hyperbolic cut originating at $+\xi_B$ and passing asymptotic to the positive imaginary axis, as indicated in Fig. 3(a). However, this branch cut violates the deformed inversion contour and is not permissible. This is as expected, since the mapping $\xi^2 = \lambda^2 - \zeta^2$ will enforce spectral behavior on nonspectral modes. Having discarded the idea of mapping the Sommerfeld-plane branch cut, any branch cutting in the $\xi$-plane can be chosen, as long as it: 1) maintains the continuity of the physical problem, and 2) does not violate the deformed inversion contour. The first consideration, when taken in conjunction with decomposition (13), forces the branch cut to approach infinity asymptotically along the negative imaginary axis, while the second consideration forces it to pass from the UHP, across the real axis, into the LHP. Any branch cut obeying the above guidelines will not separate spectral (where $\mathcal{R}e\{p_c\} > 0$) from nonspectral (where $\mathcal{R}e\{p_c\} < 0$) sheets in the $\xi$-plane. A typical choice is shown in Fig. 3b, with the improper sheet denoted by the shaded area. Locating the pole singularities must again be accomplished in a manner consistent with the $\xi$-plane cutting. The pole singularities, arising from the reflection and coupling coefficients, are associated with the natural modes of the background environment [9]. Those poles which occur on the proper sheet of the $\xi$-plane correspond to the finite number of bound surface-wave modes of the background structure, while those poles occurring on the improper sheet correspond to the leaky-wave modes of that environment.

The most significant consequence of the given branch-cut choice for leaky-wave modes is that the inversion contour remains on the top sheet of the $\xi$-plane, thus allowing for the use of techniques such as Cauchy's integral theorem to evaluate the inverse $\xi$-transforms that represent the Green's functions. The inversion contour passes

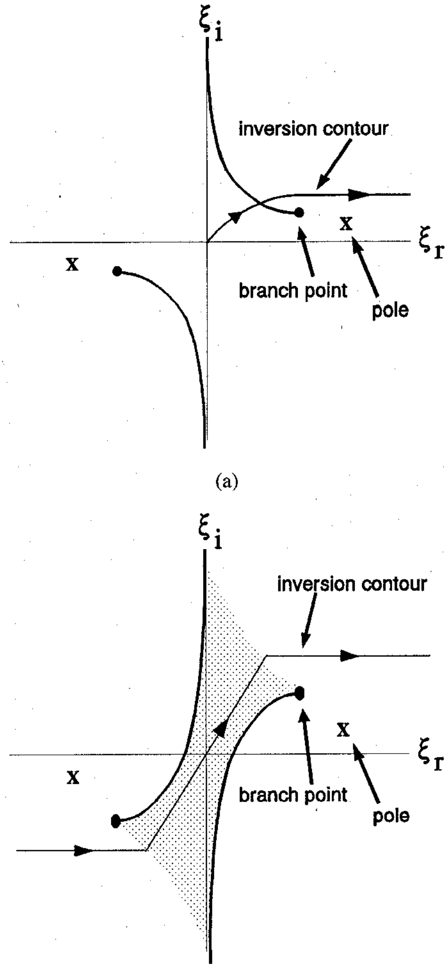


(b)

Fig. 3. (a) Map of Sommerfeld-plane branch cuts into $\xi$-plane branch cuts for leaky-wave modes, incorrectly passing through the inversion contour. (b) Typical $\xi$-plane branch cuts for leaky-wave modes. The shaded portion indicates the nonspectral region of the top sheet.

through a small portion of the nonspectral sheet of the $\xi$-plane, which introduces the nonspectral behavior of leaky modes, but always remains on the top sheet (Fig. 3(b)). This is in contrast to other work [4] in which leaky modes are found by enforcing the Sommerfeld branch cut that separates the spectral sheet from the nonspectral sheet in the $\xi$-plane, *then* allowing the inversion contour to pass through the Sommerfeld branch cut (Fig. 3(a)). While this procedure maintains convergence of the forward transform on the $x$-coordinate, the integration path passes from the top sheet to the bottom sheet and back again. It is consequently impossible to apply Cauchy's theorem. Since the integrand is not analytic, existence of the inverse transform cannot be assured, and no determination can be made of which, if any, leaky-wave poles of the background environment are implicated.

## V. Conclusions

A rationale for determining the axial radiation spectrum of microstrip transmission lines has been advanced. The branch cut in the axial transform plane, associated with the radiation spectrum, plays an important role in the evaluation of the spectral integrals on the transverse spatial frequencies, and provides a consistent methodology for locating the associated singularities. Furthermore, techniques such as Cauchy's integral theorem are applicable, as integration paths always remain on a single sheet, regardless of singularity location.

## References

[1] T. E. Rozzi, "Rigorous analysis of the step discontinuity in a planar dielectric waveguide," *IEEE Trans. Microwave Theory Tech.*, vol. MTT-26, pp. 738–746, Oct. 1978.

[2] T. E. Rozzi, L. Zappelli and M. N. Husain, "Radiation from Discontinuities in Dielectric Rib Waveguide," in *Proc. 1991 European Microwave Conf.*, Stuttgart, Sept. 1991, pp. 872–877.

[3] A. A. Oliner, "Leakage from higher modes on microstrip line with application to antennas." *Radio Science*, vol. 22, no. 6, pp. 907–912, Nov. 1987.

[4] K. A. Michalski and D. Zheng, "Rigorous analysis of open microstrip lines of arbitrary cross section in bound and leaky regimes," *IEEE Trans. Microwave Theory Tech.*, vol. 37, pp. 2005–2010, Dec. 1989.

[5] Y. Yuan and D. P. Nyquist, "Full-wave perturbation theory based upon electric field integral equations for coupled microstrip transmission lines," *IEEE Trans. Microwave Theory Tech.*, vol. 38, pp. 1576–1584, 1990.

[6] J. S. Bagby and D. P. Nyquist, "Dyadic Green's functions for integrated electronic and optical circuits," *IEEE Trans. Microwave Theory Tech.*, vol. MTT-35, pp. 206–210, Feb. 1987.

[7] A. Sommerfeld, *Partial Differential Equations in Physics.* New York: Academic Press, 1964, pp. 236–265.

[8] R. E. Collin, *Field Theory of Guided Waves.* Piscataway, N.J.: IEEE-Press, 1991. pp. 725–744.

[9] M. S. Viola, "An integral-operator approach to the electromagnetics of integrated optics," Ph.D. dissertation, Michigan State University, 1988.

[10] R. E. Collin, *Field Theory of Guided Waves.* Piscataway, N.J.: IEEE Press, 1991, pp. 824–826.

[11] W. C. Chew and J. A. Kong, "Resonance of the axial-symmetric modes in microstrip disk resonators," *J. Math. Phys.*, vol. 21, pp. 582–591, Nov. 1979.

[12] Y. Yuan, "Integral-operator analysis of layered media and integrated microstrip configurations," Ph.D. dissertation, Michigan State University, 1991.

# Characterizing the Cylindrical Via Discontinuity

Paul H. Harms, Jin-Fa Lee, and Raj Mittra

*Abstract*—**Design of efficient electronic packaging for today's high-speed digital circuits and monolithic microwave integrated circuits requires accurate characterization of the electrical discontinuities that occur because they can significantly degrade the circuit performance by introducing various effects such as capacitive and inductive loading. However, discontinuities such as the cylindrical via are difficult to characterize because its relatively complicated geometry must be accurately modeled for good results. In this work, it is demonstrated that the nonorthogonal finite-difference time-domain (FDTD) technique can handle cylindrical via discontinuities without the use of an excessive number of unknowns as would be required with an equivalent orthogonal FDTD approach. Since the FDTD analysis is band limited in the frequency domain, the inaccurate, high-frequency components need to be removed before performing reliable transient analyses with the numerical results. The use of window filters to solve this problem is discussed, and a Hanning window is employed in a study of the transient response of an equivalent circuit for the via.**

Manuscript received Jan. 28, 1992; revised May 15, 1992.

The authors are with the Electromagnetic Communication Laboratory, Department of Electrical and Computer Engineering, University of Illinois, 1406 W. Green St., Urbana, IL 61801-2991.

IEEE Log Number 9204014.

0018–9480/93$03.00 